

Article

Changes in Abrasive Wear Resistance during Miller Test of High-Manganese Cast Steel with Niobium Carbides Formed in the Alloy Matrix

Grzegorz Tęcza 

Department of Cast Alloys and Composites Engineering, Faculty of Foundry Engineering, AGH University of Science and Technology, 23 Reymonta Str., 30-059 Kraków, Poland; tecza@agh.edu.pl

Abstract: High-manganese Hadfield cast steel is commonly used for machine components operating under dynamic load conditions. The high fracture toughness and abrasive wear resistance of this steel are the result of an austenitic structure, which—while being ductile—at the same time tends to surface harden under the effect of cold work. Absence of dynamic loads (e.g., in the case of sand abrasion) causes rapid and premature wear of parts. To improve the abrasive wear resistance of high-manganese cast steel for operation under the conditions free from dynamic loads, primary niobium carbides are produced in this cast steel during the melting process to obtain in castings, after melt solidification, the microstructure consisting of an austenitic matrix and primary niobium carbides uniformly distributed in this matrix. The measured hardness of the tested samples as cast and after solution heat treatment is 260–290 HV and is about 30–60 HV higher than the hardness of common Hadfield cast steel, which is 230 HV. Compared to common Hadfield cast steel, the abrasive wear resistance of the tested high-manganese cast steel measured in the Miller test is at least three times higher at the niobium content of 3.5 wt%. Increasing the niobium content to 4.5 wt% in the tested samples increases this wear resistance even more.

Keywords: high-manganese cast steel; microstructure; primary carbides; hardness; abrasion



Citation: Tęcza, G. Changes in Abrasive Wear Resistance during Miller Test of High-Manganese Cast Steel with Niobium Carbides Formed in the Alloy Matrix. *Appl. Sci.* **2021**, *11*, 4794. <https://doi.org/10.3390/app11114794>

Academic Editor:
Joamin Gonzalez-Gutierrez

Received: 13 April 2021
Accepted: 18 May 2021
Published: 24 May 2021

Publisher's Note: MDPI stays neutral with regard to jurisdictional claims in published maps and institutional affiliations.



Copyright: © 2021 by the author. Licensee MDPI, Basel, Switzerland. This article is an open access article distributed under the terms and conditions of the Creative Commons Attribution (CC BY) license (<https://creativecommons.org/licenses/by/4.0/>).

1. Introduction

One of the best-known high-manganese alloys is Hadfield cast steel. It is named after the British metallurgist Robert Hadfield, who invented this material in 1882. It is commonly used for the production of components such as mill linings, hammers, jaws, and cones of crushers, parts of construction machines, and components used in the energy industry. It is an alloy with high wear resistance, but only under dynamic loads. When a component made of Hadfield cast steel is operated under low-load conditions, e.g., sand abrasion, its wear resistance is comparable to that of carbon cast steel [1–3]. Figure 1 compares the abrasive wear response in the Miller test of surface-hardened Hadfield cast steel and carbon cast steel with 0.4% C content.

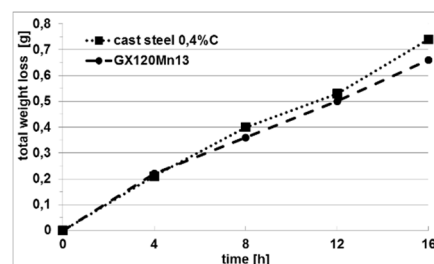


Figure 1. Abrasive wear response of surface-hardened Hadfield cast steel vs. carbon cast steel containing 0.4% C [own research].

To improve the abrasive wear response of castings made from high-manganese steel, Hadfield steel with the additions of carbide-forming elements such as chromium or molybdenum is used [1–8]. The research described in [4] shows changes in the microstructure of Hadfield cast steel with the addition of 1.4% Cr. The change in chemical composition changes the microstructure and leads to the precipitation of increased amounts of complex carbides not only at the grain boundaries but also in the interior of castings. Figure 2 shows the microstructure of such cast steel. The precipitation of a large number of carbides causes high internal stresses, which can lead to crack formation in castings during cooling in foundry mold.

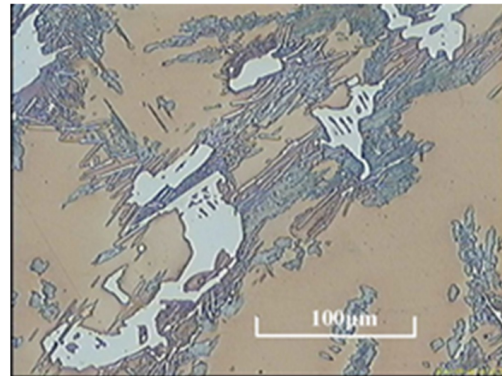


Figure 2. As-cast microstructure of Hadfield steel with the addition of chromium (1.4%); austenitic matrix with precipitates of lamellar alloyed cementite; Nital etching, [4].

Solution heat treatment of castings made from alloys with increased chromium content does not guarantee obtaining a purely austenitic structure. It is also doubtful if this structure could be obtained by other measures applied, such as higher austenitizing temperature and longer time of this treatment [4]. Figure 3 shows an example of the microstructure of Hadfield cast steel with the addition of 1.4% Cr, where after solution heat treatment at 1200 °C and annealing for 80 min, an austenitic matrix with undissolved carbides at the grain boundaries was obtained. In his own unpublished study, the author has demonstrated that the addition of chromium in an amount of 1.4% causes in the Miller test a two times lower weight loss of the tested samples compared to Hadfield cast steel with typical chemical composition subjected to standard heat treatment. The wide use of Hadfield cast steel in industry drives the constant search for modifications of its properties through changes in the chemical composition. For example, the research described in [5,6] shows changes in the microstructure and abrasive wear resistance in the Miller test of Hadfield cast steel with the addition of 5.5% V. Owing to the change in chemical composition, in the solution heat-treated test castings, an austenitic matrix with faceted vanadium carbides evenly distributed in this matrix was obtained. Figure 4 shows the microstructure of this alloy. The uniform distribution of vanadium carbides in the alloy matrix improves the abrasive wear resistance in the Miller test at least two times in the as-cast condition and three times after solution heat treatment. Figure 5 compares the abrasive wear response of Hadfield cast steel in the as-cast condition and after solution heat treatment with that of high-manganese cast steel containing 5.5% V.

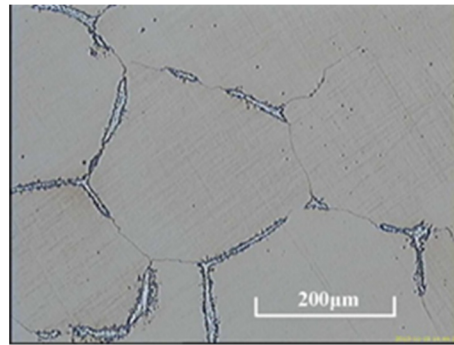


Figure 3. Microstructure of Hadfield cast steel with the addition of chromium (1.4%) after solution heat treatment with water quenching (1200 °C/80 min); austenitic matrix with undissolved carbides visible at the grain boundaries; Nital etching, [4].

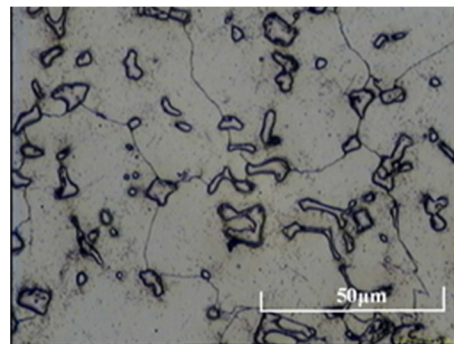


Figure 4. Microstructure of high-manganese cast steel with the addition of 5.5% V after solution heat treatment with water quenching, Nital etching, [6].

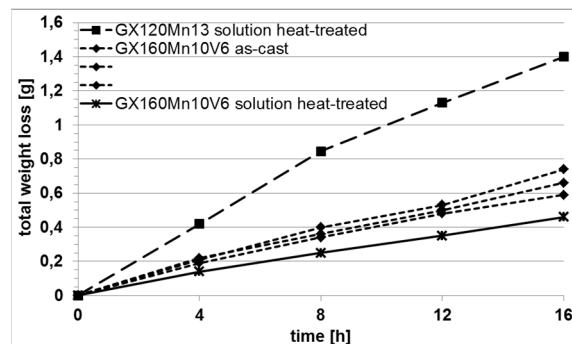


Figure 5. Abrasive wear response of Hadfield cast steel vs. high-manganese cast steel with the addition of 5.5% V, [6].

Research works on the properties of Hadfield cast steel with the addition of titanium are also available. Studies [7,8] show changes in the microstructure of Hadfield cast steel containing titanium (0.4–2.5% Ti) and in its abrasive wear resistance in the Miller test. In all the tested samples after solution heat treatment, the obtained structure consisted of an austenitic matrix and primary titanium carbides evenly distributed in this matrix with absence of grain-boundary cementite. Figure 6 shows sample microstructure of this alloy with 2.0% Ti content. In the Miller test of abrasive wear resistance, the wear resistance was at least twice as high as in common Hadfield cast steel. Figure 7 compares the abrasive wear response of Hadfield cast steel with that of high-manganese cast steel containing the addition of Ti.

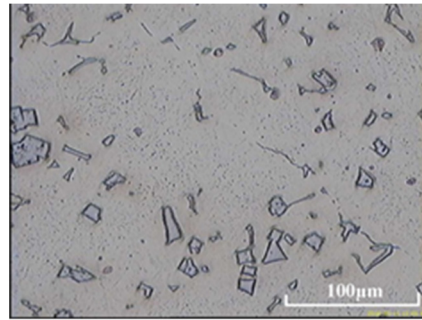


Figure 6. Sample microstructure of alloy with the addition of 2.0% Ti after solution heat treatment; austenitic matrix with primary titanium carbides evenly distributed in this matrix; Nital etching, [7].

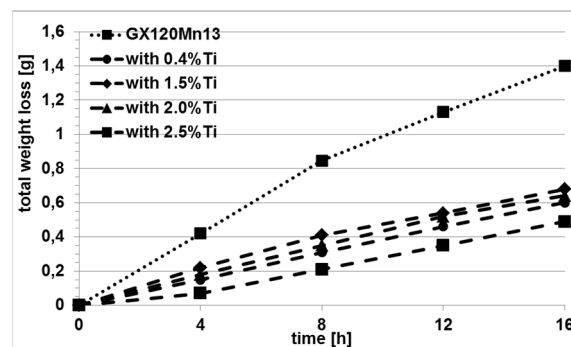


Figure 7. Abrasive wear response of Hadfield cast steel vs. high-manganese cast steel with the addition of 0.4–2.5% Ti, [8].

The satisfactory results obtained so far in studies of the changes in microstructure and abrasive wear resistance in the Miller test have prompted the author to undertake a research on the high-manganese cast steel with niobium additions.

2. Materials and Methods

Specimens were cut out from the test “Y”-type ingots with a wall thickness of 25 mm and a weight of about 8 kg, cast from the steel melted in a 30 kg capacity induction furnace. Carburizer in the form of Fe-Nb60 ferroalloy and electrolytic manganese were added to molten steel in the metallurgical process to supplement the chemical composition. The addition of niobium resulted in the formation of primary niobium carbides in the steel melt. After casting solidification, these carbides were distributed in the alloy matrix.

Chemical analysis of the tested alloys was carried out under industrial conditions using a Foundry Master spectrometer and was next completed with laboratory examinations using an energy dispersive X-ray fluorescence spectrometer. Table 1 shows the chemical composition of the tested alloys.

Table 1. Chemical composition of the tested high-manganese cast steel.

Alloy Designation	Chemical Composition [wt%]										
	C	Mn	Si	P	S	Cr	Ni	Mo	V	Ti	Nb
MnNb_3	1.7	14.0	1.1	0.05	0.02	1.0	0.6	0.1	0.03	0.05	3.5
MnNb_4	1.6	14.1	0.8	0.02	0.02	1.4	0.6	0.2	0.02	0.03	4.5

Compared to traditional Hadfield cast steel, the tested cast steel was characterized by an increased content of carbon (1.6–1.7%) and manganese (14.0–14.1%), and by chromium

content (1.0–1.4%) resulting from the presence of this element in the charge. Niobium content in the test castings was at a level of 3.5 and 4.5%.

The cut-out specimens were subjected to solution heat treatment from 1050 °C with water quenching. The annealing time was 40 min.

Hardness tests were performed with a Vickers hardness tester under a load of 30 kg.

Microstructures of the test alloys were examined using a Neophot 32 light microscope equipped with a camera for digital image recording.

Chemical analysis of the composition of carbides and matrix of the tested alloys was performed using a JSM-7100F scanning microscope equipped with an EDS microanalyzer.

Phases present in the tested samples were identified with a Kristalloflex 4H X-ray diffractometer from Siemens using the characteristic Cu radiation ($K\alpha = 0.154$ nm) with a step size of 0.05 2 theta/1 s.

The abrasive wear response was determined in the Miller test, which is used to compare the abrasive wear behavior of various construction materials. This method allowed the author to compare the previously obtained results with the results obtained by other members of the research team [5,6,8–14]. The test specimens with dimensions of 25.4×12.7 mm and a thickness of 9 mm were placed in the holders of the device under a constant load of 22.2N and were next subjected to abrasion process in a water—silicon carbide mixture in 1:1 ratio. The counter-sample was the rubber lining of the trough bottom where the abrasion process took place. Silicon carbide with grain number 220 according to FEPA standard and grain size 53–73 μ m was used. Sixteen-hour abrasive wear tests were performed in 4 cycles. Every four hours, the samples were weighed with an accuracy of 0.001 g. Based on the obtained values of mass losses, abrasive wear curves were plotted for the tested samples. The values of wear obtained for the samples of the tested alloys were compared with the values of wear obtained for the reference sample made of Hadfield cast steel with 1.2% C, 13% Mn, and 0.8% Si, subjected to standard solution heat treatment from the temperature of 1050 °C.

The surface of the samples after abrasive wear test was macroscopically compared with the surface of the Hadfield cast steel sample.

3. Test Results and Discussion

Table 2 gives parameters of the heat treatment carried out on the tested samples and on the reference sample. The results of hardness measurements are also included. Solution heat treatment with water quenching of the tested alloys from the temperature of 1050 °C has only a minor effect on the hardness values compared to as-cast samples. The measured hardness of the tested samples as cast and after solution heat treatment is about 260–290 HV and is about 30–60 HV higher than the hardness of traditional Hadfield cast steel, which is 230 HV.

Table 2. Heat treatment of the tested samples and their hardness.

Alloy Designation	Heat Treatment	Hardness [HV]
MnNb_3	As cast	291, 295, 289, 289, 295, 294, 290, 290, 293, 294
	1050 °C/40 min/water quenching	276, 283, 289, 276, 289, 285, 282, 287, 280, 277
MnNb_4	As cast	295, 291, 293, 291, 295, 294, 295, 293, 291, 293
	1050 °C/40 min/water quenching	262, 257, 262, 281, 265, 268, 275, 277, 271, 269,
GX120Mn13	1050 °C/water quenching	230, 227, 229, 230, 227, 228, 227, 229, 230, 230

Based on the results obtained by light microscopy (Figure 8) and scanning electron microscopy (Figure 9), analysis of the chemical composition of carbides (Figure 10 and Table 3), surface distribution of elements such as Nb, Fe and Mn in the area of visible carbides (Figure 11), and X-ray phase examinations (Figure 12), it was found that the microstructure of the examined alloys after solution heat treatment consists of an austenitic matrix and primary niobium carbides. Carbides visible on the cross-sections of the metallographic specimens are evenly distributed in the austenitic matrix and partially also occur in the form of small clusters (Figures 8 and 9).

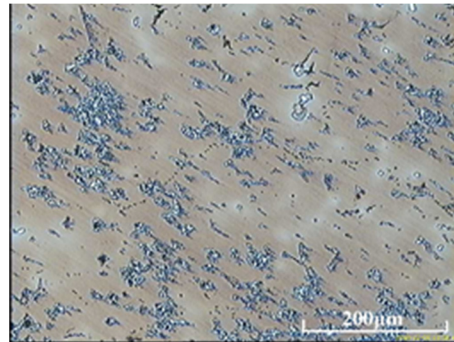


Figure 8. Sample microstructure of alloy with the addition of 4.5% Nb after solution heat treatment; austenitic matrix with niobium carbides, Nital etching.

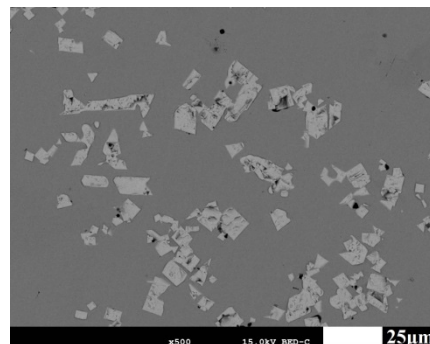


Figure 9. Sample scanning image of alloy with the addition of 4.5% Nb after solution heat treatment; austenitic matrix with niobium carbides, unetched sample.

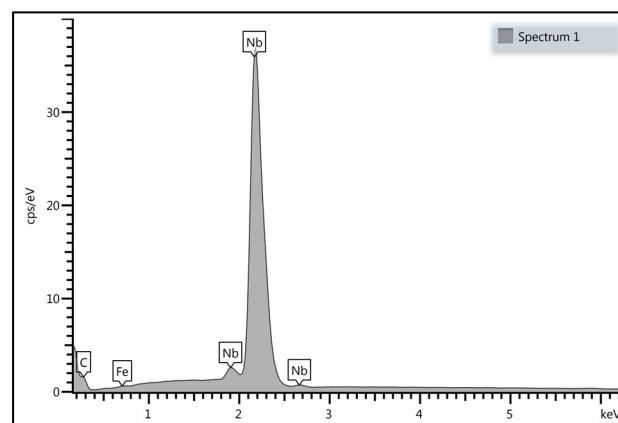
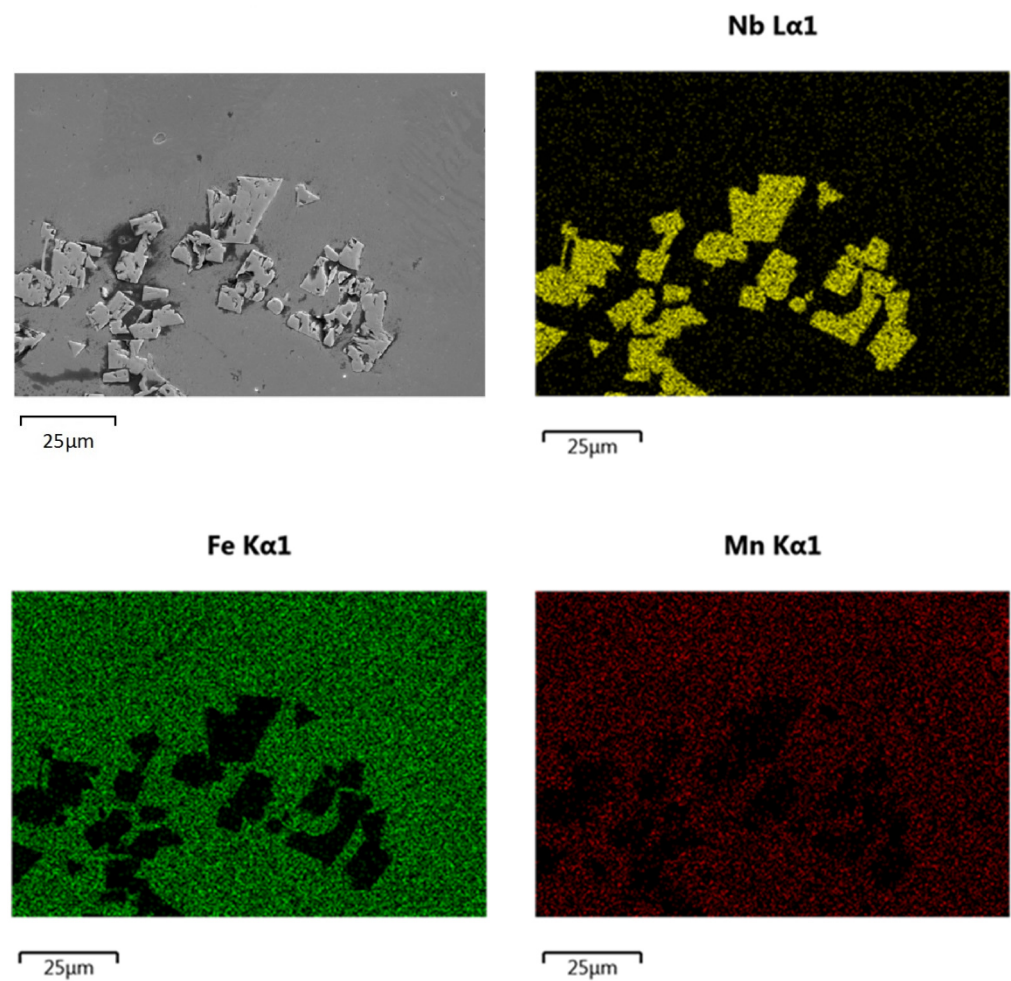


Figure 10. Energy spectrum obtained by EDS from the visible niobium carbide precipitates.

Table 3. Chemical composition in microregions of the alloy matrix and carbides.

Place of Analysis	[wt%]						
	Si	Ti	Cr	Mn	Fe	Nb	Other
carbide	–	0.6	–	–	2.6	94.9	rest
	–	0.8	–	–	1.7	91.2	rest
	–	–	–	–	1.4	92.8	rest
matrix	1.1	–	0.7	13.5	84.7	–	rest
	1.2	–	1.0	16.4	8.4	–	rest
	1.3	–	0.5	15.4	81.4	–	rest

**Figure 11.** Surface distribution of Nb, Fe, and Mn in the area of niobium carbides.

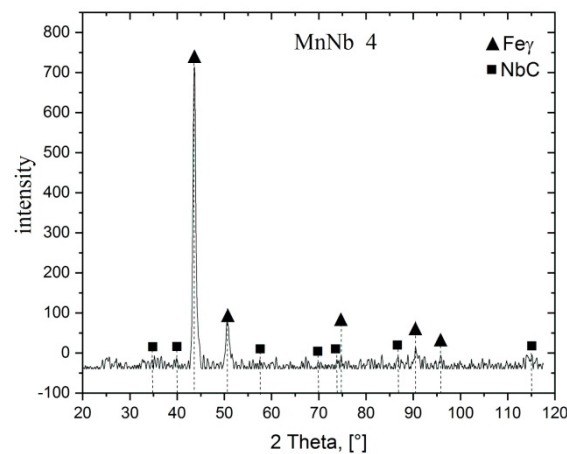


Figure 12. X-ray diffraction pattern of alloy with the addition of 4.5% Nb.

Based on the results of Miller test, a diagram was drawn up in Figure 13 showing total weight loss of the tested samples as a function of abrasion time. From this diagram it follows that the abrasive wear resistance of the tested high-manganese cast steel is at least 3 times higher than the abrasive wear resistance of Hadfield cast steel. The addition of 3.5% Nb to the alloy reduces the wear rate from 1.4 g/16h to 0.461 g/16h. With the niobium content of 4.5%, the wear rate is even lower and amounts to 0.366 g/16h, which gives a nearly four times higher value of the abrasive wear resistance.

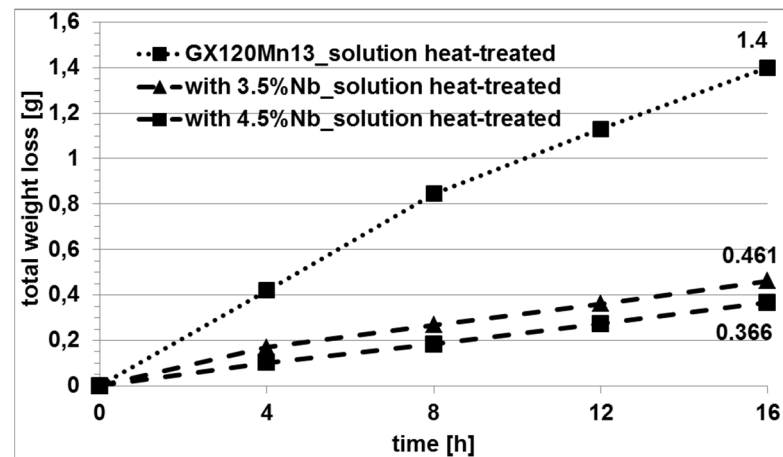


Figure 13. Abrasive wear response of Hadfield cast steel vs. tested high-manganese cast steel with Nb addition.

Some differences were also observed in the surface topography of samples subjected to abrasion test. The results are shown in Figure 14. The surface of Hadfield cast steel shows deep scratches and grooves with embedded abrasive particles (Figure 14a). The addition of niobium makes the wear of the samples more uniform (Figure 14b,c). The surface of the samples is even, the grooves and scratches disappear, and niobium carbides formed in the structure are protruding from the alloy matrix.

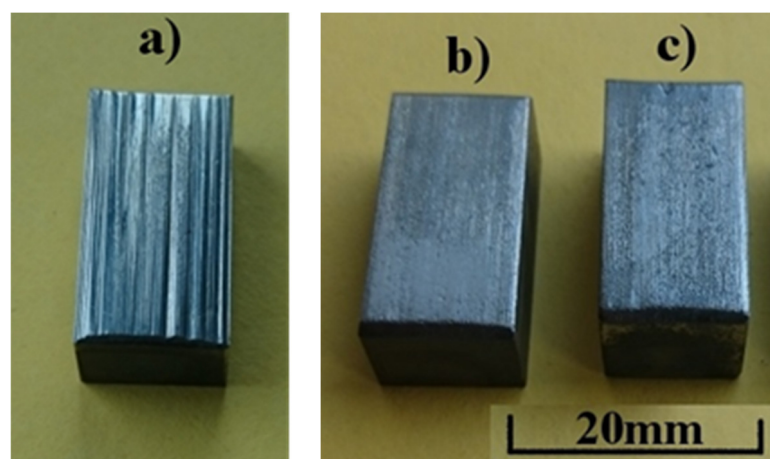


Figure 14. Surface of samples after abrasion test: (a) reference sample of Hadfield cast steel, (b) high-manganese cast steel with the addition of 3.5% Nb, (c) high-manganese cast steel with the addition of 4.5% Nb.

Improving the properties of Hadfield cast steel is one of the major research trends related to its use in industry. The introduction of Ti, V or Nb additives allows increasing the abrasive wear resistance owing to the formation of carbides in the alloy matrix. However, as the quoted data shows, in all cases, the carbides occur in the form of polyhedra with sharp edges. This carbide morphology may increase the tendency of castings to crack formation by increasing the level of stresses on the carbide-alloy matrix phase boundary. Therefore, the development of a melting technology of high-manganese cast steel which would produce oval or spheroidal carbides after melt solidification would be highly desirable.

4. Conclusions

The following conclusions can be drawn from the research carried out:

1. The hardness of the tested samples in both as-cast condition and after solution heat treatment is about 260–290 HV which means that it is about 30–60 HV higher than the hardness of Hadfield cast steel.
2. The microstructure of the tested alloys after solution heat treatment consists of an austenitic matrix and primary niobium carbides evenly distributed in this matrix.
3. The abrasive wear resistance of the tested high-manganese niobium-containing cast steel is at least 3 times higher than that of Hadfield cast steel.
4. The addition of Nb makes the sample wear uniform without any furrows and scratches.

Funding: This research received no external funding.

Institutional Review Board Statement: Not applicable.

Informed Consent Statement: Not applicable.

Conflicts of Interest: The author declares no conflict of interest.

References

1. Kniaginina, G. *Austenityczne Staliwo Manganowe (Austenitic Manganese Cast Steel)*; PWN: Kraków, Poland, 1968.
2. Smith, R.W.; DeMonte, A.; Mackay, W.B.F. Development of high-manganese steels for heavy duty cast-to-shape applications. *J. Mater. Process. Technol.* **2004**, *153–154*, 589–595. [[CrossRef](#)]
3. Głownia, J. *Odlewy ze Stali Stopowej—Zastosowanie (Castings from Alloy Steel—Applications)*; Fotobit: Kraków, Poland, 2002.
4. Tęcza, G.; Sobula, S. Effect of heat treatment on change microstructure of cast high-manganese hadfield steel with elevated chromium content. *Arch. Foundry Eng.* **2014**, *14*, 67–70.
5. Głownia, J.; Tęcza, G.; Asłanowicz, M.; Ościłowski, A. Tools cast from the steel of composite structure. *Arch. Metall. Mater.* **2013**, *58*, 803–808. [[CrossRef](#)]

6. Tęcza, G.; Głownia, J. Resistance to abrasive wear and volume fraction of carbides in cast high-manganese austenitic steel with composite structure. *Arch. Foundry Eng.* **2015**, *15*, 129–133. [[CrossRef](#)]
7. Tęcza, G.; Garbacz-Klempka, A. Microstructure of cast high-manganese steel containing titanium. *Arch. Foundry Eng.* **2016**, *16*, 163–168. [[CrossRef](#)]
8. Tęcza, G.; Zapała, R. Changes in impact strength and abrasive wear resistance of cast high manganese steel due to the formation of primary titanium carbides. *Arch. Foundry Eng.* **2018**, *18*, 119–122.
9. Głownia, J.; Kalandyk, B.; Camargo, M. Wear resistance of high Cr-Ni alloys in iron ore slurry conditions. *Inżynieria Mater.* **2002**, *5*, 694–697.
10. Kalandyk, B.; Zapała, R. The abrasive wear behaviour of alloy cast steel in SiC-water slurry. *Arch. Foundry Eng.* **2009**, *9*, 91–94.
11. Kalandyk, B.; Zapała, R. Effect of high-manganese cast steel strain hardening on the abrasion wear resistance in a mixture of SiC and water. *Arch. Foundry Eng.* **2013**, *13*, 63–66. [[CrossRef](#)]
12. Kasinska, J.; Kalandyk, B. Effects of Rare Earth Metal Addition on Wear Resistance of Chromium-Molybdenum Cast Steel. *Arch. Foundry Eng.* **2017**, *17*, 63–68. [[CrossRef](#)]
13. Kalandyk, B.; Tęcza, G.; Zapała, R.; Sobula, S. Cast High-Manganese Steel—the Effect of Microstructure on Abrasive Wear Behaviour in Miller Test. *Arch. Foundry Eng.* **2015**, *15*, 35–38. [[CrossRef](#)]
14. Tęcza, G.; Nitkiewicz, Z.; Głownia, J. Porównanie odporności na ścieranie staliwa po obróbce cieplnej z przetopieniem powierzchni (Comparison of the abrasive wear resistance of cast steel after heat treatment with surface remelting). In *Nowe Technologie i Osiągnięcia w Metalurgii i Inżynierii Materiałowej, Proceedings of the VI Międzynarodowa Konferencja Naukowa: Nowe Technologie i Osiągnięcia w Metalurgii i Inżynierii Materiałowej (VI International Scientific Conference on New Technologies and Achievements in Metallurgy and Materials Engineering)*, Częstochowa, Poland, 2 June 2005; Wydaw.WIPMiFS PC: Częstochowa, Poland, 2005; Volume 2, pp. 622–627.